Available online at www.sciencedirect.com
SciVerse ScienceDirect
Energy Procedia 16 (2012) 1033 – 1040
Energy Procedia

2012 International Conference on Future Energy, Environment, and Materials

A Flexible Endoscopic Machining Tool

Yang Lei[a*], Yuhua Cheng[a], Scott F. Miller[b] *

[a]School of Automation, University of Electronic Science and Technology of China, No.2006, Xiyuan Ave., Chengdu 611731, China
[b]Department of Mechanical Engineering, University of Hawaii at Manoa, Honolulu, HI 96822, USA

Abstract

Flexible endoscopic tools are considerably applied in industrial image based inspecting operations, but none of them are currently effective enough to carry out machining tasks, such as grinding. If machining and inspection can be done in a single step, significant amount of labor force, money and energy can be saved in industrial repairing and maintenance tasks. This paper proposed a concept design of novel endoscopic machining tool, which aims at quantitatively and precisely removing material from imperfect components in hard-to-reach cavities, such as turbine blades in a jet engine. Prediction models are built to estimate the pose, force and material removal rate (MRR) of a modified PENTAX ES-3801 endoscope. Preliminary experimental results show that in two-dimensional (2D) grinding configuration the MRR average error of 22% has been achieved for 18 samples tested. In the end, concept designs of self-stabilized endoscopic grinding tool are proposed and discussed.

Keywords: Material removal; Endoscopic tool; Machining

1. Introduction

1.1. Motivation and Objective

Many applications in industrial and medical image based inspection make considerable use of flexible endoscopes to gain visual access to holes, hollows and cavities that are difficult to enter and examine. Industrial endoscopes are used to inspect the inner part of a hard-to-reach area such as the interior of a jet engine, as shown in Fig. 1(a). The endoscope uses fiber optics and powerful lens systems to provide lighting and transmit the interior image to be viewed. Fig. 1(b) shows cracks, V-shaped nicks and impact

* Corresponding author. Tel.: +8618224406883.
E-mail address: leiyang.uestc@gmail.com.

 doi:10.1016/j.egypro.2012.01.165

found along the leading edge of a jet engine turbine blade. When imperfections are discovered during a maintenance operation, in order to prevent such notches or nicks from becoming more pronounced and potentially cracking the turbine blade, it is desirable to detect them early and, if possible, repair or blend the defects [1].

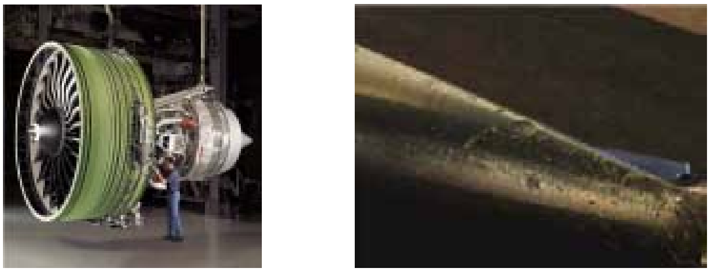

Fig. 1. (a) GE90 aircraft engine[2]; (b) cracked turbine blade[3]

There is currently no effective way to quantitatively remove material from internal components of engineered cavities. Current machine tools have a relatively massive base and are considered to be a sufficiently rigid system, i.e., the deflection of the machining base and tools are negligible and the MRR can be easily quantified from the tool movement. However, these tools are too big and inflexible for machining tasks in small cavities and hard-to-reach areas. A major need is to be able to inspect and remove a known amount of material with application specified precision from the blade of a turbine engine, such as those used in aircraft or power plants, during a maintenance operation without having to undertake time consuming and therefore expensive dismantling and reassembly [4].

For smoothing jet engine turbine blade cracks, a good accuracy of material removal is believed to be a fraction of 0.001 mm3 to 1.0 mm3 in volume or 0.004 mg to 4.0 mg in mass (densities of Nickel, Titanium, and Aluminum are 8.91, 4.56 and 2.70 g/cm3 respectively), which sets the target of accuracy for endoscopic machining [5, 6]. In current practice to repair damaged blades, the engine must be removed, dismantled, repaired and reassembled back, requiring up to 850 hours of labor and costing as much as $500,000[7]. If success, the proposed endoscopic tool will be able to detect interior flaws of a complex structure and perform a machining operation (grinding, polishing, deburring, etc.) to repair them in a single step, which will save significant amount of labor force, money and energy in industrial repairing and maintenance tasks.

1.2. Background of Endoscopic Machining Tools

Endoscopic tools have been patented for blending or smoothing defects on a turbine blade [5, 8], however these instruments are not built for quantitative material removing and the machining process can only be monitored by visual means, which is imprecise and inadequate [4]. In Moeller et al.'s design [8], as shown in Fig. 2(a) the grinding head was fixed by articulating an outer portion of the support tube. Desgranges et al. [5] patented a tool supported by exterior means as shown in Fig. 2(b). Both of the patented instruments seem to have been designed for specific applications and have shortcomings. Firstly, the operation is imprecise, i.e., the amount of material removal and positioning are not known. Secondly, the material removal can only be estimated qualitatively by visual means. The fixturing methods are limited to either external or application specific. Thirdly, the depth of penetration into the cavity seems to be limited to less than 1 m in most cases.

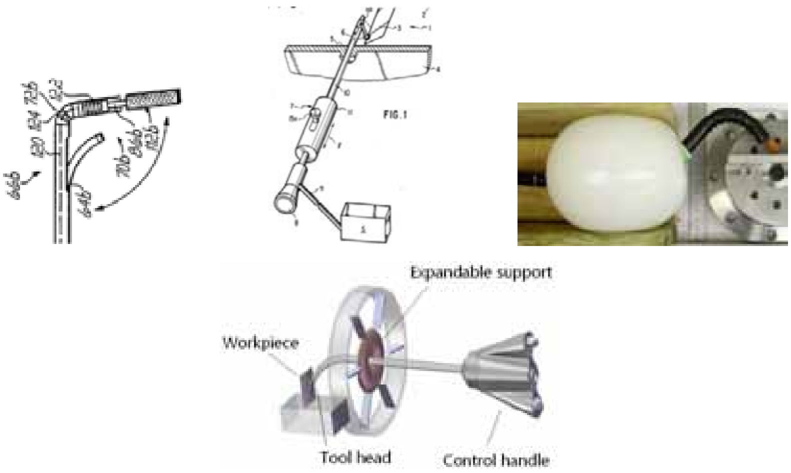

Fig. 2. (a) patented endoscopic grinding tool [8]; (b)patented tool [5]; (c) concept drawing of endoscopic machining scenario; (d) endoscopic grinding tool supported by balloon fixture

Fig. 2(c) shows the concept and setup of proposed endoscope machining. The flexible, inflatable fixture supports the base of endoscope bending section against the cavity. A small grinding tool is connected to and driven by an external motor through a flexible steel cable. In the Fig. 2(d), a balloon is inflated to fix the bending section against the cavity wall and an aluminum workpiece is fixed on a dynamometer that measures machining forces.

The ultimate goal of this research is to build up an efficient and precise endoscopic machining tool, which will substitute current inefficient rigid tools by consuming less energy, labor force and money in machining tasks. Section two presents the methodology and experimental setup for the instrumented endoscope. Sensors were installed onto the endoscope and geometric model was built to study the kinetic characteristics of the bending section. Energy based MRR models was described. In Section three, endoscopic machining results are presented and the MRR error of the endoscopic grinding experiment is calculated and analyzed. Sections four discusses current technique hurdles of endoscopic machining and proposed some novel and feasible tool head design solutions.

2. Model Description and Experimental Setup

2.1. Pose/Force Estimation Model and Sensor Setup

A PENTAX ES-3801 endoscope was partially disassembled and instrumented with a linear variable differential transformer (LVDT) displacement sensor and a load cell for measurement of the displacement and force on the driving cable, as shown in Fig. 3(a). The endoscope is fixed on a table at point B and it can be controlled in the two dimensional plane by the driving cable pairs. Estimated position and orientation were derived only by the readouts of the LVDT sensor and the load cell in our approach. The estimated position of endoscope bending section was defined as point E(x,y), estimated orientation was defined as angle $\angle EAR$ or vector direction EH . The predicted machining force was exerted by a spring scale at point E and was assumed to be always perpendicular to vector EH.

To track the actual or "true" position and orientation of the tip of the endoscope in real-time, a computer vision technique called object tracking was set up. The camera system can be seen in Fig. 3(a) and the output from the customized computer software can be seen in Fig. 3(b). Red markers were attached at crucial points on the endoscope and independently tracked for verification of the estimation method.

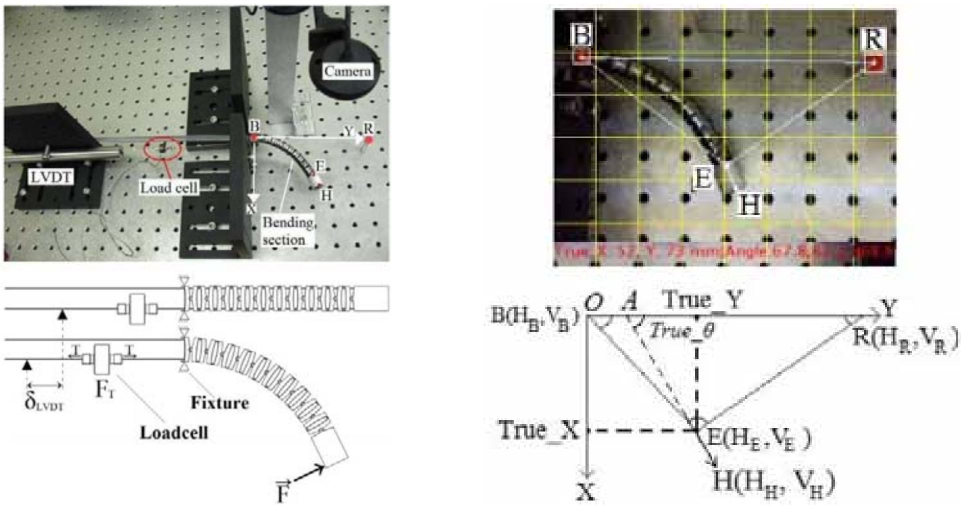

Fig. 3. (a) Experimental setup of endoscope instrumented with LVDT sensor and load cell (top view); (b) endoscopic tool pose acquired by object tracking technique as a reference

In the experiment, the bending section was bent and locked to an arbitrary position E(x, y) by the driving cable. Then a known external force (Fext) was applied perpendicular to the tip point, E, of the endoscope. This force would push point E to a new position, E(x', y'), and the orientation angle ∠EAR would changed as well. The readouts of LVDT sensor and load cell were input into a pose estimation model and a force prediction model to estimate the position of point E, orientation angle ∠EAR and external force applied on point E. The governing equations of endoscope tool head are given by Eq. (1), (2).

$$X_{est} = \sum_{i=2}^{N}\left[L\sin\left(\sum_{j=1}^{i}\frac{\theta_{free}}{N} - \Delta\theta'_j\right)\right],\ Y_{est} = L + \sum_{i=2}^{N}\left[L\cos\left(\sum_{j=1}^{i}\frac{\theta_{free}}{N} - \Delta\theta'_j\right)\right],\ \theta_{est} = \theta_{free} - \sum_{i=2}^{N}\Delta\theta'_i \tag{1}$$

$$\Delta\theta'_i = \Delta\theta_i - \left(\sum_{j=1}^{i-1}\dot{\Psi}_{ij}\cdot\Delta\theta_j + \sum_{j=i+1}^{N}\dot{\Psi}_{ij}\cdot\Delta\theta_j\right),\ \sum_{j=1}^{i-1}\dot{\Psi}_{ij} + \sum_{j=i+1}^{N}\dot{\Psi}_{ij} = 1\,(j\in[1..N]) \tag{2}$$

2.2. MRR Prediction Model and Material Removal Measurement

An endoscopic grinding operation was performed on an aluminum workpiece and the MRR model estimated the mass of material that was removed by the driving cable force and position inputs. The workpiece was weighed before and after the endoscopic grinding operation for comparison. One group of endoscopic grinding experiments was conducted to find the parameters in the semi-empirical material removal prediction model, as shown in Eq. (3), (4) and Table 1. The Es are energy values designated by their subscripts. Another two groups of endoscopic grinding experiments were performed to validate the repeatability of the MRR prediction model.

$$M_{removal} = \kappa(E_s) = \kappa(E_{grind} - E_{overhead} - E_{chatter})$$
$$= \kappa T f_{grind} \left\{ \left[\mu(\delta_{LVDT}, F_{cell}) G(\delta_{LVDT}, F_{cell}) \cdot \pi D - \int_{-\theta}^{+\theta} P_B(\theta) d\theta - E_f \right] \cdot \left[1 - R(P_{cell}) \right] \right\} \tag{3}$$

$$E_{chatter} = \left(E_{grind} - E_{overhead}\right) \cdot R(P_{cell}) = \left(E_{grind} - E_{overhead}\right) \cdot \left(1 - \frac{\int_{f_1^-}^{f_1^+} \lambda_1 P_1(f) df}{\sum_{i=1}^{N} \int_{f_i^-}^{f_i^+} \lambda_i P_i(f) df} \right) \tag{4}$$

Endoscopic grinding experiment setup is shown in Fig. 4(a). The dynamometer is fixed onto an optical table and the workpiece is fixed on top of the dynamometer. The endoscope bending section can bend freely in horizontal workspace XOY but is restricted vertically. The base point O of the bending section is fixed between two metal brackets. The workpieces were cut from AISI 6061-T651 aluminum bar and each piece is 8 ×38 ×95 mm in size and 74 - 76 g, approximately. The initial bending angle θ was about 90 degrees and grinding angle was set to zero, which means the grind stone was in full contact with the surface of the workpiece. For each grinding test, the motor was set to 5000 rpm (83.3 Hz).

During the test the horizontal control knob was turned to bend the bending section and create the force between the grinding tool and workpiece. The turning force was quickly increased to a preset level and the control knob was locked, and from that moment material was being removed. After 30 seconds of grinding, the control knob was unlocked and turned counter clockwise to lift the grinding stone off the surface rapidly. Before and after grinding, each workpiece was weighed on a Mettler Toledo XP504 precision scale with 0.1 mg resolution (readability). The decreased value of weight of the i^{th} workpiece was recorded as M_i. Fig. 4(b) shows two grinding marks on sample #8 (smoother) and #9 (more chatter).

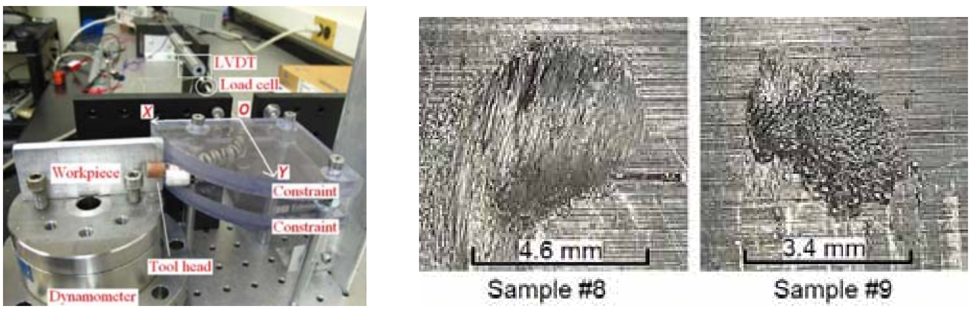

Fig. 4. (a) Setup of 2D endoscopic grinding experiment for MRR model validation; (b) grinding marks on aluminum workpieces

3. Experimental Results and Conclusion

Eighteen aluminum workpieces were machined and weighed for the Experiment 2 and 3 data. The average error between the estimated and measured weight was 22%, and the standard deviation was 10.33%, as shown in Fig. 5. This error is high compared to what is required for precise applications, and was affected by backlash and low tolerance of the commercially available endoscope of the current study. However, the results are adequate to prove the concept of flexible machining.

Table 1. MRR model parameters

Parameter	Symbol	Value
Force ratio	μ	1.2*cos(|θ-1.815|)
Chatter coefficients	$\lambda1$	1.0
	$\lambda2$	0.9
	$\lambda3$	20
Overhead coefficients	$\alpha3$	0.08
	$\beta3$	90
Energy coefficient	κ	1.3E-03

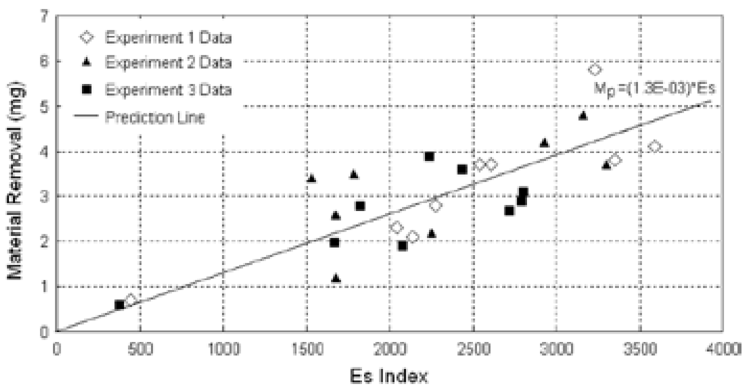

Fig. 5. Comparison of amount of material removed by MRR model estimation with experimental results

4. Concept Designs and Discussion

On one hand, machining tasks such as grinding and cutting are force critical processes and hence require the tool heads be well supported by the tool structures. On the other hand, an endoscopic tool bearing a highly flexible body structures can provide very limited supporting force to the tool head. In this case, the future of flexible endoscopic tools shall benefit from but not limited to self-stabilized tool head designs.

Fig. 6 is a proposed design, in which two grinding wheels are setting in a frame and driven by motor running in opposite directions. It is an intuitive self-stabilized design. Although two machining forces (shown as two white arrows) might not be able to completely nullify each other due to workpiece surface conditions, the whole structure should be more stable than traditional one-way grinder.

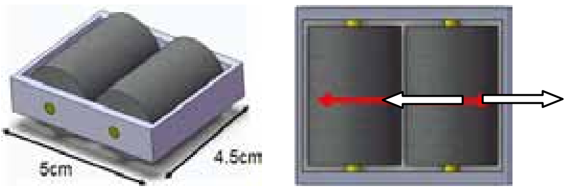

Fig. 6. (a) Actuator design using traditional motor (3D view); (b) Top View (Motor not show in picture)

Fig. 7 demonstrates a grinder structure. Three rectangular cross sectional grinders are constrained in a tool frame by six piezoelectric actuators. When phase shifted driven signals are acting on the piezoelectric actuators, these grinders will be moving to opposite directions at any given moment. Therefore the grinding forces (friction forces between grinders and workpiece), shown as three white arrows in Fig. 7 (a), can be controlled to balance each other out.

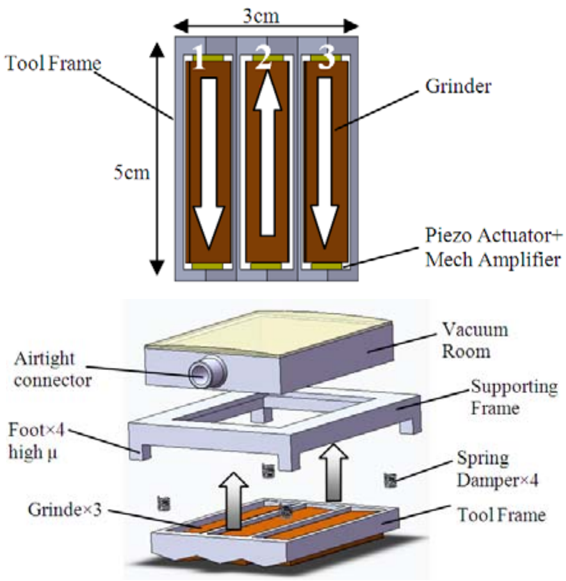

Fig. 7. (a) Grinding Tool Design; (b) A Self-Stabilized Grinding Tool (Arrows show air flow direction.)

Acknowledgement

This work is partially supported by the Specialized Research Fund for the Doctoral Program of Higher Education of China (20100185120005) and Visiting Scholarship of State Key Laboratory of Power Transmission Equipment & System Security and New Technology (Chongqing University) (2007DA10512711415) and the National Natural Science Foundation of China (Grant No. 61102141).

References

[1] Moeller. Grinding apparatus for blending deffects on turbine blades and associated method of use, May 2005.

[2] The advent of a better jet engine. Web, October 2007. URL http://www.defenseindustrydaily.com/the-advent-of-a-better-jet-engine-03623/. as referenced on 2/8/2009.

[3] Tim J. Carter. Common failures in gas turbine blades. *Engineering Failure Analysis*, 12(2):237–247, April 2005. doi: 0.1016/j.engfailanal. 2004.07.004.

[4] Diener. Instrument for working the surfaces of parts inside engineered cavities, December 1995.

[5] Desgranges. Apparatus for retouching, in situ, components such as the rotor blades of a turbomachine, and a retoughing, method using the appraratus., April 1992.

[6] Silvia Seng. Turbine engine fan disk crack detection test. *Final Report DOT/FAA/AR-04/28*, Naval AirWarfare Center,Weapons Division,Weapons Survivability Laboratory, China Lake, CA, September 2004.

[7] Pratt & Whitney. Pratt & whitney wins maintenance contract for rolls-royce engines on harrier fighters. *Technical report*, 2002. URL http://www.pw.utc.com/media_center/press_releases/2002/07_jul/7-21-2002_8512115.asp.

[8] Moeller. Grinding apparatus for blending deffects on turbine blades and associated method of use, May 2005.